

# Positron-Electron Annihilation

Carl Akerlof  
March 8, 2010

## 1. Introduction

This experiment attempts to explore several features of positron-electron annihilation. One of the attractive aspects of  $e^+e^-$  annihilation is the relative simplicity of the interaction. To first order, the two-body system decays into two back-to-back photons, each carrying an energy of  $m_e c^2$ . This feature has provided the basis for a medical imaging technique called Positron Emission Tomography (PET). PET is often used in conjunction with other tomographic techniques such as MRI to image potentially cancerous tumors in which exploratory surgery would be particularly hazardous. In condensed matter, the interactions between positronium and the substrate can provide information about the details of the substrate structure via the effects on the momentum distribution at the instant of annihilation. The angular distributions measured in this experiment will be used to estimate the typical momenta associated with these systems. This is not quite trivial because the angles are typically of the order of a few milliradians (fractions of a degree).

## 2. Physics of positronium production and decay

The source for positrons in this experiment is a radioactive source,  $^{22}\text{Na}$ , with an activity of about  $5 \mu\text{C}$ .  $^{22}\text{Na}$  has a half-life of 2.6019 years and decays with the release of 2842.3 KeV. 90.3% of the decays emit a  $\beta^+$  with a 545.7 KeV maximum kinetic energy followed by a 1274.5 KeV gamma-ray transition to the  $^{22}\text{Ne}$  ground state. Approximately 0.06% of the time, the  $\beta^+$  emission bypasses the excited state and directly transitions to the  $^{22}\text{Ne}$  ground state. About 10% of all decays proceed by electron capture instead. The total energy budget is satisfied by including the 511.0 KeV rest mass carried off by the Na valence electron that is now unbound. The positrons from these processes travel a certain

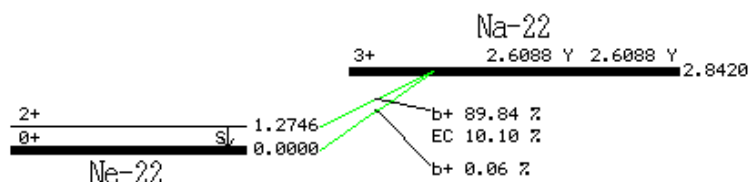


Figure 1. Nuclear energy levels for  $^{22}\text{Na}$  decay to  $^{22}\text{Ne}$ . (taken from <http://atom.kaeri.re.kr/cgi-bin/decay?Na-22 EC>)

distance, slowing down by Coulomb interactions with neighboring atoms. Ultimately, they meet with an electron and form a hydrogenic-like atom called positronium which will decay with greatest probability when the two leptons are in an S-state. If the spins are anti-parallel (para-positronium), the annihilation will occur via two photons with a lifetime of 124 ps. If the spins are parallel (ortho-positronium), angular momentum

conservation and Bose-Einstein statistics require three-photon final states with a considerably longer lifetime of 142 ns. Calculations and measurements of these lifetimes have a long history here at the University of Michigan positron group, now led by Professor David Gidley. The comparison of these values for ortho-positronium has been used as a significant test of quantum electrodynamics (QED). The experiment described below looks only at para-positronium annihilation.

## 2. Positron-electron annihilation experimental equipment

The equipment for this experiment consists primarily of a pair of scintillators and photomultipliers (PMTs) rigidly mounted on an 8' long aluminum rail. A steel box placed midway between the two detectors is designed to hold the  $^{22}\text{Na}$  radioactive source so that the relative angle between detected photons can be easily varied by moving the source position in a direction perpendicular to the line separating the photomultipliers. The transverse location of the source is controlled by a 1" micrometer screw. Two steel spacer rods, 0.90" and 1.80" long, extend the range of displacements (see Figure 3). For most of the measurements, the direction of the detected photons must be collimated to less than 1/8" (3 mm). This is accomplished with two sets of small tungsten blocks that should be mounted in the vertical supports attached to the aluminum rail. A single high voltage power supply (Power Designs 1570A) provides power to the PMTs via a Zener diode voltage divider which can vary the potential applied to the two tubes by as much as several hundred volts. Note that the PMTs are wired for POSITIVE high voltage. **Never operate the power supply above 1700 volts!** The logic diagram for the 2- $\gamma$  event detection is shown in Figure 2 below. An Ortec model 871 Timer & Counter module is available to control count durations. The interval is selected by the *Inc M* and *Inc N* switches on the front panel. The output of this unit gates the discriminators through connections to the NIM crate. A reset pulse to the Jorway 1880C scalers is generated automatically by depressing the *Start* button. For most of the measurements, counting

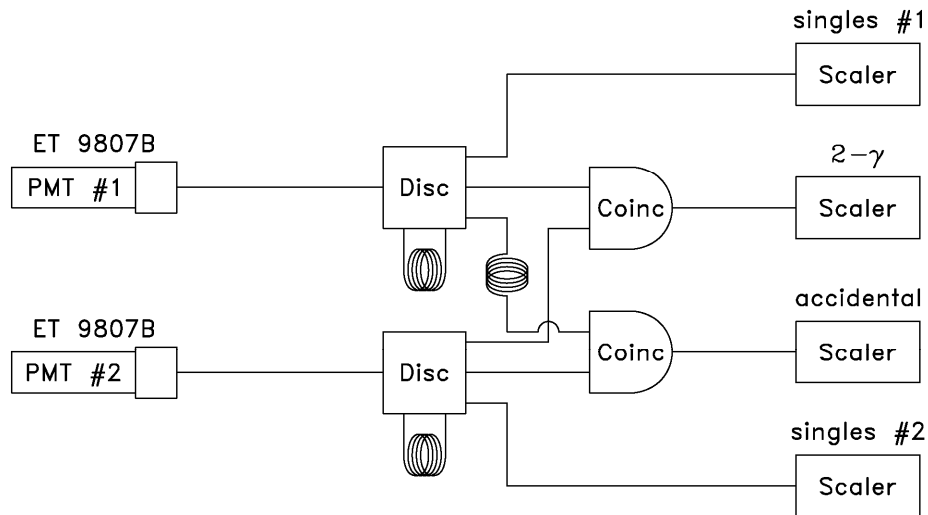


Figure 2. Schematic diagram for the detection of 2- $\gamma$  positronium annihilation.

durations of several minutes are required to obtain sufficient statistics. In February 2010, the photomultipliers were replaced with new tubes which operate at lower voltages and thus less noise. This has simplified the electronics and reduced background.



Figure 3. Spacer blocks for source displacement measurement and collimator width alignment. From left to right: 1.80" steel spacer rod, 0.90" steel spacer rod, 0.75 and 2.50 mm collimator alignment tool, 10.0 mm collimator alignment tool, 0.010" collimator alignment tool.

### 3. Exploring the spatial distribution of the positronium annihilations

A critical aspect of this experiment is the spatial localization of the positrons when they annihilate with electrons. If this is highly dispersed, it will be much more difficult to measure the angular distribution of the two photons produced in the decay. Such dispersal arises from two effects: (1) the radioactive material,  $^{22}\text{Na}$ , is distributed over a finite volume within the sample holder and (2), the  $\beta^+$  from the  $^{22}\text{Na}$  decay travels a finite distance from its parent nucleus before annihilation. These effects can be measured or at least estimated by observing the 2- $\gamma$  coincidence rate with the apparatus arranged as shown in Figure 4 below.

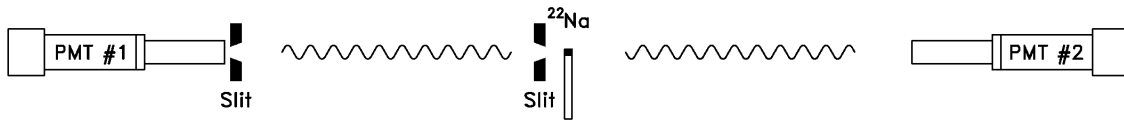


Figure 4. Arrangement of collimation slits to determine the  $\beta^+$  spatial distribution within the  $^{22}\text{Na}$  source holder.

With slit aperture nearest the  $^{22}\text{Na}$  source set to  $\frac{1}{4}$  mm, the distribution within the source holder can be determined to similar accuracy. The geometry is shown schematically in Figure 5.

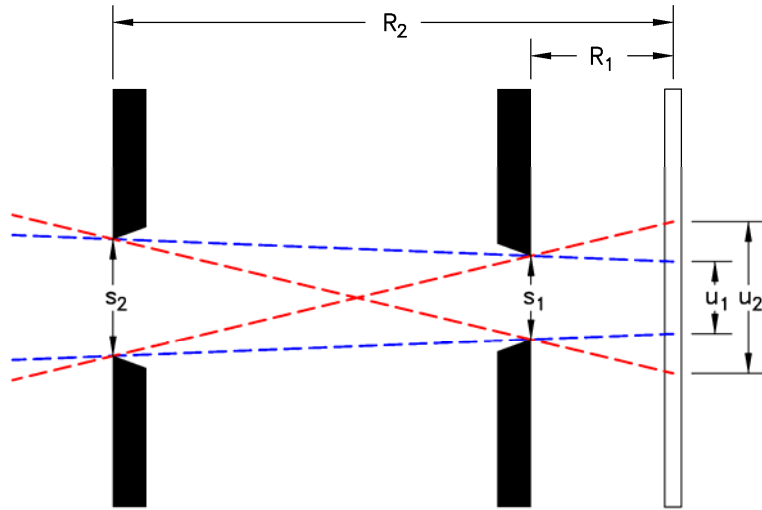


Figure 5. Extrapolation of rays to the  $^{22}\text{Na}$  radioactive source holder on the right. Gamma-rays from the region between the two blue lines are accepted with uniform probability. Above and below the red lines, no rays can be detected. Between the red and blue lines, the acceptance rises linearly from zero to the maximum value.

From the diagram above, it is easy to show that:

$$u_1 = \frac{|R_2 s_1 - R_1 s_2|}{R_2 - R_1}$$

$$u_2 = \frac{R_2 s_1 + R_1 s_2}{R_2 - R_1}$$

Since the collimation acceptance function is trapezoidal with width  $u_1$  at the top and width  $u_2$  at the base, the full width at half maximum (FWHM) is:

$$u_{1/2} = \frac{1}{2} (u_1 + u_2) = \frac{R_2}{R_2 - R_1} s_1$$

As long as  $R_1$  is a small fraction of  $R_2$ , the resolution along the longitudinal axis of the source holder is just slightly larger than the slit width,  $s_1$ . It is a good idea to make  $s_2$  larger than  $s_1$  to maintain a high coincidence counting rate and thus improve the statistical accuracy of your measurements. However, if the slit width,  $s_2$ , is overmatched, ie.  $s_2/R_2 > s_1/R_1$ , the accuracy of extrapolation to the source location decreases with no improvement in the number of detected  $\gamma$ -rays. To find the proper scale for a useful value of  $s_1$ , independently estimate the projected distance that the  $\beta^+$  will travel before coming to a stop. If the range for the maximum energy  $\beta^+$  is  $d_{\text{max}}$ , the projected RMS distance will be approximately  $\frac{1}{3}d_{\text{max}}$ . The factor of  $\frac{1}{3}$  comes from the combined effects of averaging over both the positron direction and its kinetic energy distribution. The total RMS extent

of the positronium annihilation loci is the sum in quadrature of the  $^{22}\text{Na}$  source distribution and the  $\beta^+$  range.

For the measurements outlined above, the slit width for the collimator near the photomultiplier assembly should be set to 10 mm (see Figure 6). For the slit assembly adjacent to the  $^{22}\text{Na}$  source, use a spacing of 0.010" (see Figures 7a and 7b). Note that the tungsten blocks are beveled at a  $2^\circ$  angle to ensure that the geometry is cleanly defined. This makes proper orientation an important issue.

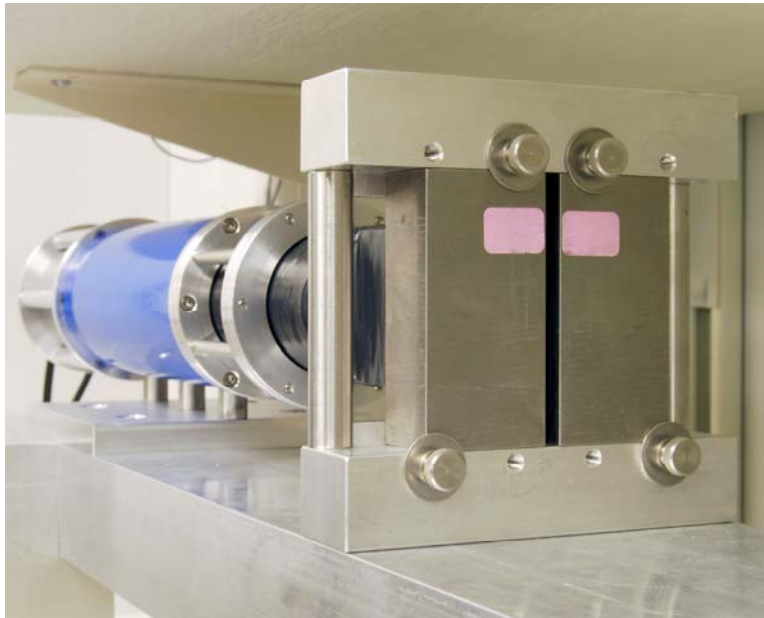


Figure 6. Tungsten slits and photomultiplier assembly. Note paper tape labels that indicate correct orientation of the W blocks.

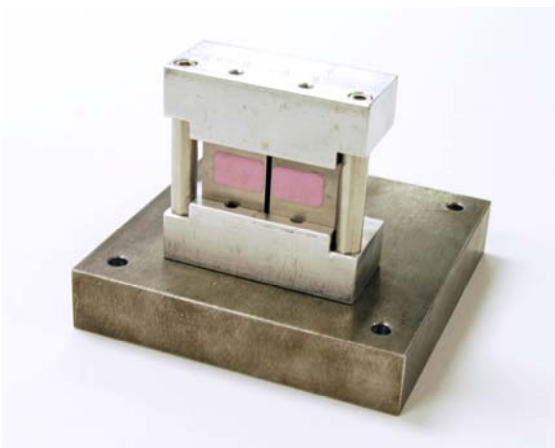


Figure 7a. Front slit assembly.

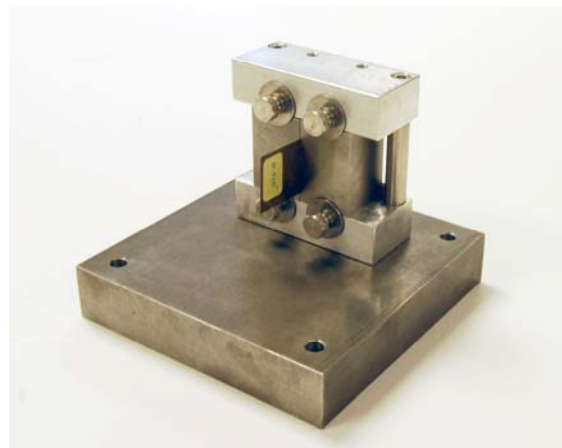


Figure 7b. Front slit assembly showing use of 0.010" width gauge.

#### 4. Collimation of the detected $\gamma$ -rays

As stated in the introduction, the relative direction of the two detected  $\gamma$ -rays must be determined with a resolution of a few milliradians. This is accomplished by placing the small tungsten collimation blocks directly in front of the detectors as shown in Figure 8 below.



Figure 8. Arrangement of collimation slits to determine the  $\gamma$ - $\gamma$  angular distribution function. The  $\gamma$ - $\gamma$  angle is varied by moving the  $^{22}\text{Na}$  source in the horizontal plane.

With the slits arranged as shown above, we need to calculate how well this system defines the  $\gamma$ - $\gamma$  angle. That can be inferred from Figure 9 below. The logic is similar to what was discussed in the previous section. The acceptance is defined in terms of the two limiting values for  $\psi_1$  and  $\psi_2$ :

$$\psi_1 = \frac{|s_1 - s_2|}{R}$$

$$\psi_2 = \frac{s_1 + s_2}{R}$$

The natural choice is to make  $s_{12} \equiv s_1 = s_2$  so that the acceptance FWHM width is  $s_{12}/R$ . This angle corresponds to a lateral motion of  $\frac{1}{2}s_{12}$  for the  $^{22}\text{Na}$  source.

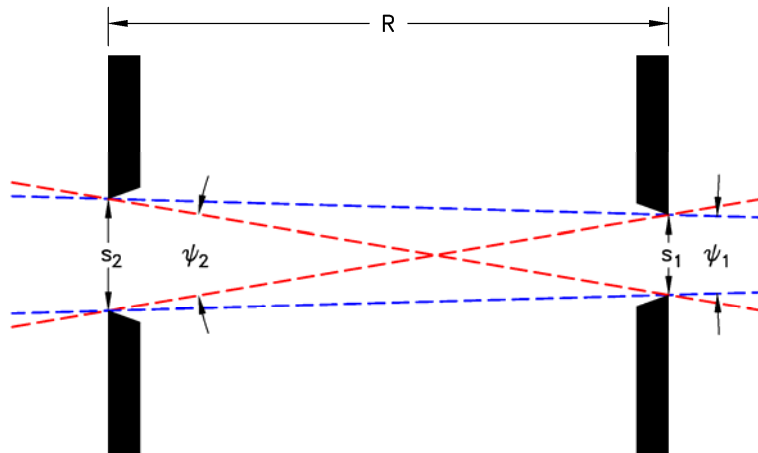


Figure 9. Collimation accuracy for 2- $\gamma$  events originating in the  $^{22}\text{Na}$  radioactive source (not shown). Gamma-rays in the region between the two blue lines are accepted with uniform probability. Above and below the red lines, no rays can be detected. Between the red and blue lines, the acceptance rises linearly from zero to the maximum value.

For these measurements, good angular accuracy is critical. Adjust the slit width in front of both photomultipliers to 2.50 mm using the appropriate spacer gauge (see Figure 3).

## 5. Kinematics of positronium annihilation

In the following, we wish to explore how the angular distribution of  $\gamma$ -rays is affected by the momentum of the positronium at the instant of annihilation. The energies of the two quanta are designated  $E_1$  and  $E_2$ . The photon with  $E_1$  is assumed to travel precisely along the  $-z$  axis (see Figure 10 below) while the other photon makes an angle,  $\psi$ , with the  $+z$  axis. The positronium has a momentum,  $P_{\pm}$ , in a direction specified by the angle,  $\theta$ . Momentum conservation requires that the directions of the positronium and the two photons are coplanar. Our aim is to find out how the angle  $\psi$  reflects the positronium momentum. To keep the notation simpler, the velocity of light will be set equal to 1.

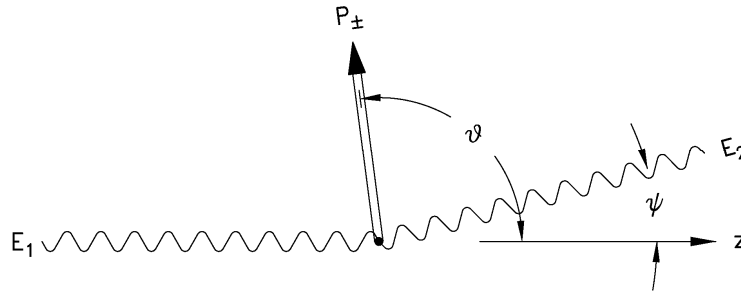


Figure 10. Kinematics of para-positronium annihilation.

The kinematic quantities describing positronium annihilation are constrained by energy conservation:

$$E_{\pm} \equiv \sqrt{P_{\pm}^2 + 4m^2} = E_1 + E_2$$

and momentum conservation:

$$P_{\pm} \cos(\theta) = -E_1 + E_2 \cos(\psi)$$

$$P_{\pm} \sin(\theta) = E_2 \sin(\psi)$$

We can explicitly solve for  $E_1$  and  $E_2$  in terms of  $P_{\pm}$  and  $x \equiv \cos(\theta)$ :

$$E_1 = \frac{2m^2}{E_{\pm} + P_{\pm}x}$$

$$E_2 = \frac{2m^2(E_{\pm} + P_{\pm}x) + P_{\pm}^2 E_{\pm}(1 - x^2)}{E_{\pm}^2 - P_{\pm}^2 x^2}$$

This leads to an explicit expression for the  $\gamma$ - $\gamma$  correlation angle,  $\psi$ , in terms of  $P_{\pm}$  and  $x$ :

$$y \equiv \sin(\psi) = \sqrt{1-x^2} \frac{P_{\pm}}{E_2}$$

Since the values of  $P_{\pm}$  that we will explore are relatively small, this previous equation can be expanded in a power series in  $P_{\pm}/m$ , a ratio less than 0.01 for all conditions of interest:

$$y \cong \left\{ \frac{P_{\pm}}{m} + \frac{x}{2} \left( \frac{P_{\pm}}{m} \right)^2 + \frac{-3+4x^2}{8} \left( \frac{P_{\pm}}{m} \right)^3 + \dots \right\} \sqrt{1-x^2}$$

To keep the description simple, only the leading term will be retained. As you might suspect, corrections to this approximation are too small to be detected. If the positronium momentum is fixed at a specific value of  $P_{\pm}$ , the two photons will be correlated so that with one photon along the  $-z$  axis, the other will be confined to a bright ring around the  $+z$  axis with angular radius,  $\psi = P_{\pm}/m$  as shown in Figure 11 below. Furthermore, with the slit geometry used in this experiment, one would expect to observe a constant count rate as the angle between the detectors is varied from  $-P_{\pm}/m$  to  $+P_{\pm}/m$ . This result is the basis for relating the experimentally observed angular distribution to the positronium momentum distribution. Assume that  $\Delta N$  events are associated with the range of positronium momenta between  $P_{\pm}$  and  $P_{\pm} + \Delta P_{\pm}$ . These will produce an increase in counts at the angle,  $\psi$ , where  $\sin(\psi) = P_{\pm}/m$ . Since the effect of these events will be distributed uniformly over the interval,  $[-P_{\pm}/m, +P_{\pm}/m]$ , the effect on the angular distribution will be an increment,  $\Delta I = -\Delta N / (2\psi)$ . Thus, we obtain:

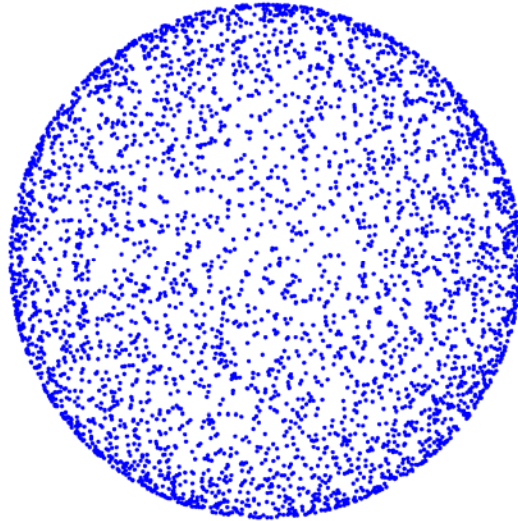


Figure 11. Monte Carlo simulation of the directional pattern for the second photon from  $e^+e^-$  annihilation assuming a unique value for  $P_{\pm}$  with the first photon directed exactly along the  $-z$  axis. Note that the density of points is greatest near the edge of the distribution. This distribution has an interesting mathematical property: any long slit will uncover the same number of events no matter how it is placed as long as the circle subtends the slit width.

$$\frac{dN}{dP_{\pm}} \propto -\psi \frac{dI}{d\psi}$$

To find a first order estimate of the momentum distribution, one can fit the experimental data to a Gaussian error distribution and then carry out the mathematical operation described above. More sophisticated numerical techniques are available to deal with more complex data.

## 6. Experimental guidelines

- a) Check that the electronic logic is wired as shown in Figure 2. With the  $^{22}\text{Na}$  source in place, check that the PMT high voltages are adjusted to count coincidences efficiently yet maintain a low enough singles rate that random coincidences are not a problem. Remember that the PMT voltages must be positive and should not exceed about 1700 volts. For these tests, remove any shielding between the detectors and the source – you want to have reasonably high rates and geometry is not crucial. Measure the coincidence rate as a separate function of the voltage on each PMT. There should be a reasonably broad plateau region where the rate is relatively independent of voltage. When you have found satisfactory values, determine the singles rates in both detectors, both with and without the radioactive source in place. The random coincidence rate is given by:

$$R = \tau N_1 N_2$$

where  $N_1$  and  $N_2$  are the singles rates in each tube in counts per second and  $\tau$  is the coincidence resolving time. The resolving time is the sum of the durations of the logic pulses from the two discriminator circuits, about 20 ns. Verify this by checking with an oscilloscope.

- b) Demonstrate the approximate back-to-back distribution of annihilation  $\gamma$ -rays by measuring the coincidence rate as a function of the longitudinal position of the  $^{22}\text{Na}$  source. Plot the results and determine the half-width of the curve.
- c) Estimate the range of the positron from  $^{22}\text{Na}$  decay, projected along the long axis of the Lucite source holder. Measure the apparent longitudinal distribution of positronium decays using the technique outlined in section 3. The counting rates will be low so make sure that the random coincidences are a small fraction of the true rate. Include a plot of the coincidence rate as a function of source position as well as an estimated width.
- d) Using the technique described in section 4, measure the  $\gamma$ - $\gamma$  angular correlation function. From the geometry of your equipment and the results from part (b), decide whether or not the angular width of the coincidence curve is consistent with exactly back-to-back  $\gamma$ -ray emission or requires additional consideration of the kinematics of the positronium at the instant of annihilation. Include a plot of

the angular distribution function as a function of source position or, better yet, as a function of the  $\gamma$ - $\gamma$  angle.

- e) If part (d) shows some evidence of positronium motion, estimate the typical momentum values from the width of your curve as described in section 5. With this information, calculate the typical kinetic energy of the positronium system at the time of annihilation and compare to atomic electron binding energies. What would be the characteristic width of the 2- $\gamma$  angular distribution if the positron annihilated immediately after emission from the  $^{22}\text{Na}$  nucleus?
- f) In the introduction, the use of positron annihilation for medical imaging was mentioned. From the calculations and measurements you have performed so far, you should be able to estimate the inherent accuracy of such a technique. You can assume that biological tissue is basically carbon with a density of about  $1 \text{ gm/cm}^3$ . Comment on the imaging resolution, the size of detectors, etc.

The following plots show data and analysis for this experiment.

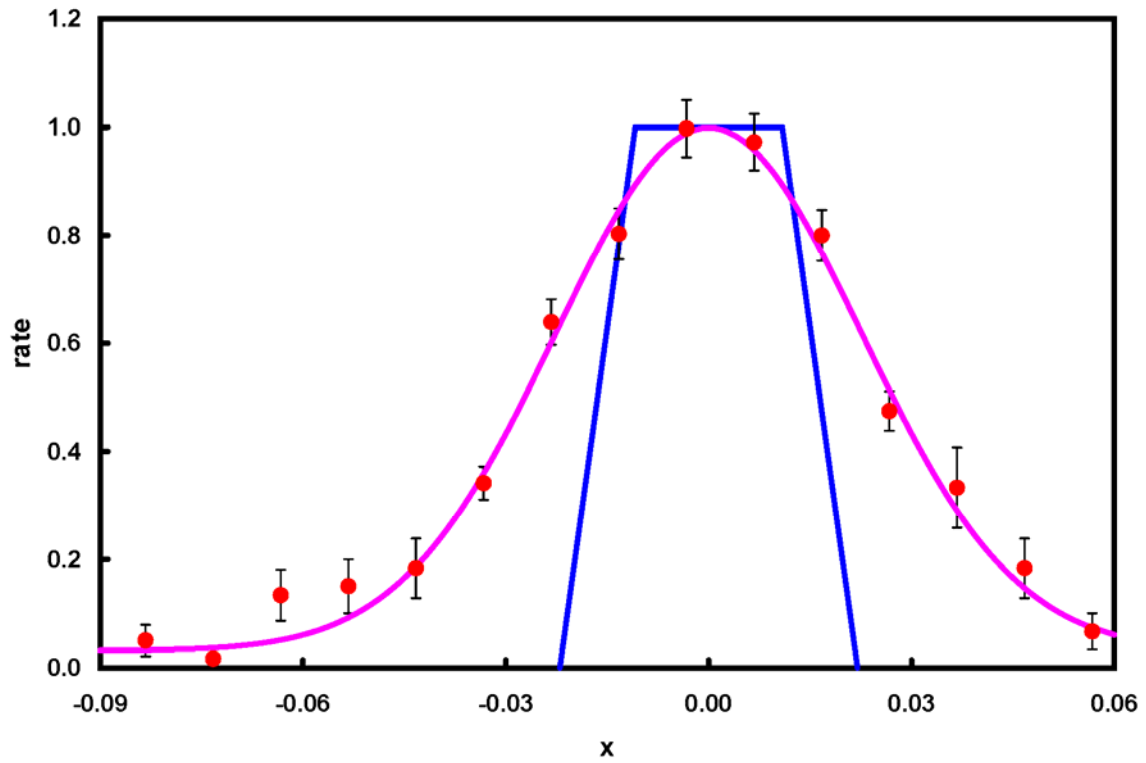


Figure 12. Counting rate with tungsten slits arranged to determine the transverse distribution of the  $e^+$  annihilations. The blue trapezoid shows what would be expected if this distribution were a  $\delta$ -function. The magenta curve is a Gaussian fit to the actual data.

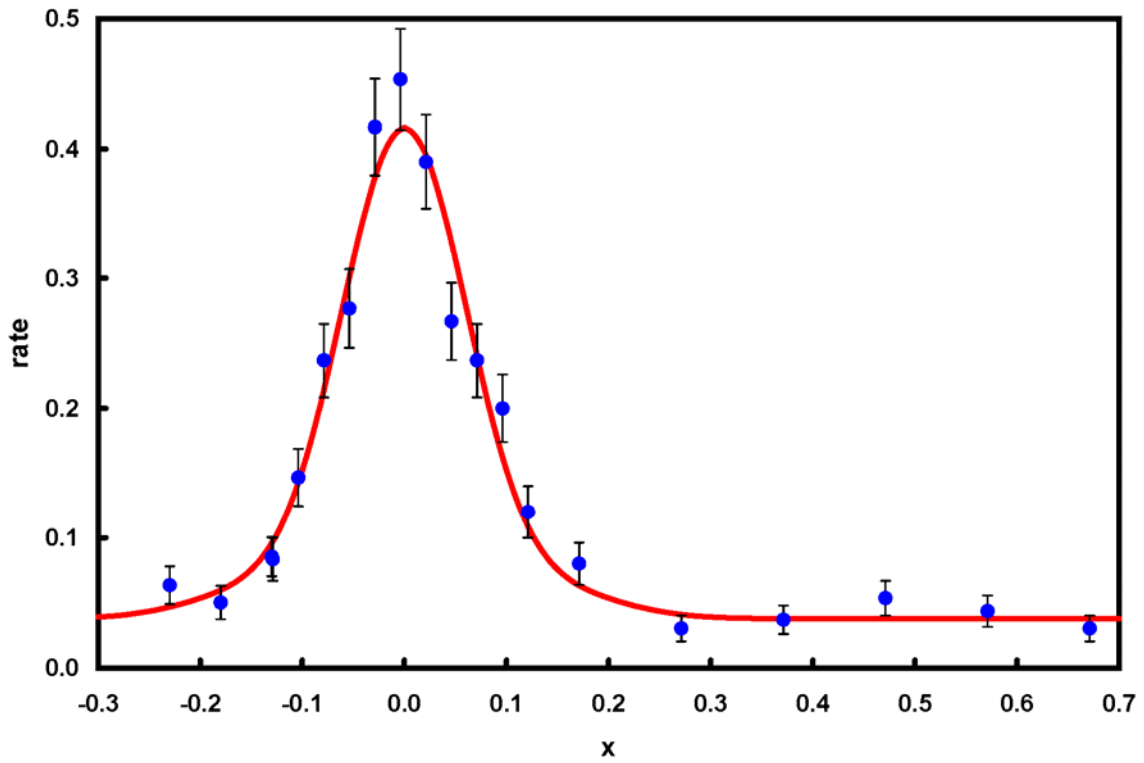


Figure 13. Two- $\gamma$  coincidence rate as a function of the source position. The red line shows a fit that includes a constant background and the first three symmetric Hermite polynomials.

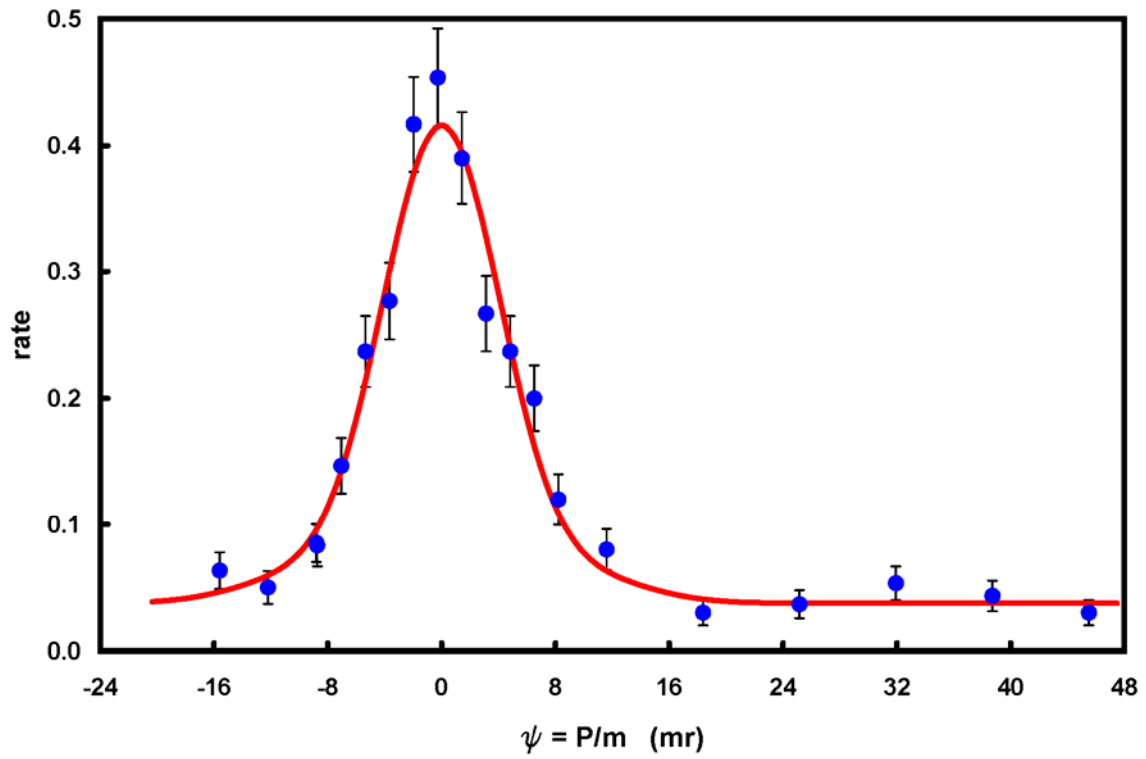


Figure 14. Two- $\gamma$  coincidence rate plotted as a function of angle (in milliradians) between source and detectors.

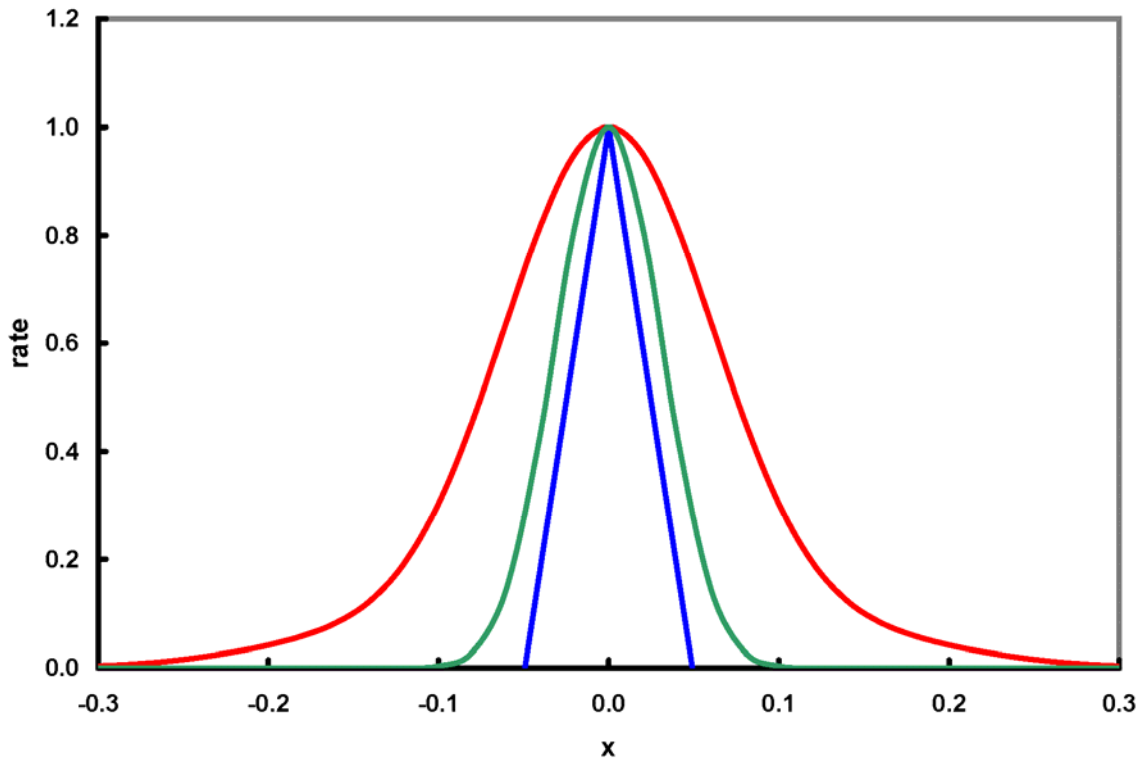


Figure 15. Estimation of effects of the extended distribution of  $e^+$  annihilations and finite slit widths. The triangular blue graph shows what would be expected for a  $\delta$ -function distribution for the  $e^+$  annihilation region. The green curve depicts the result of convolving the apparent spatial region shown in Figure 9 with the tungsten slit geometry. The red curve shows the fit to the actual 2- $\gamma$  coincidence rate. The difference between the red and green curves is due to the finite momenta of the positronium systems at decay.

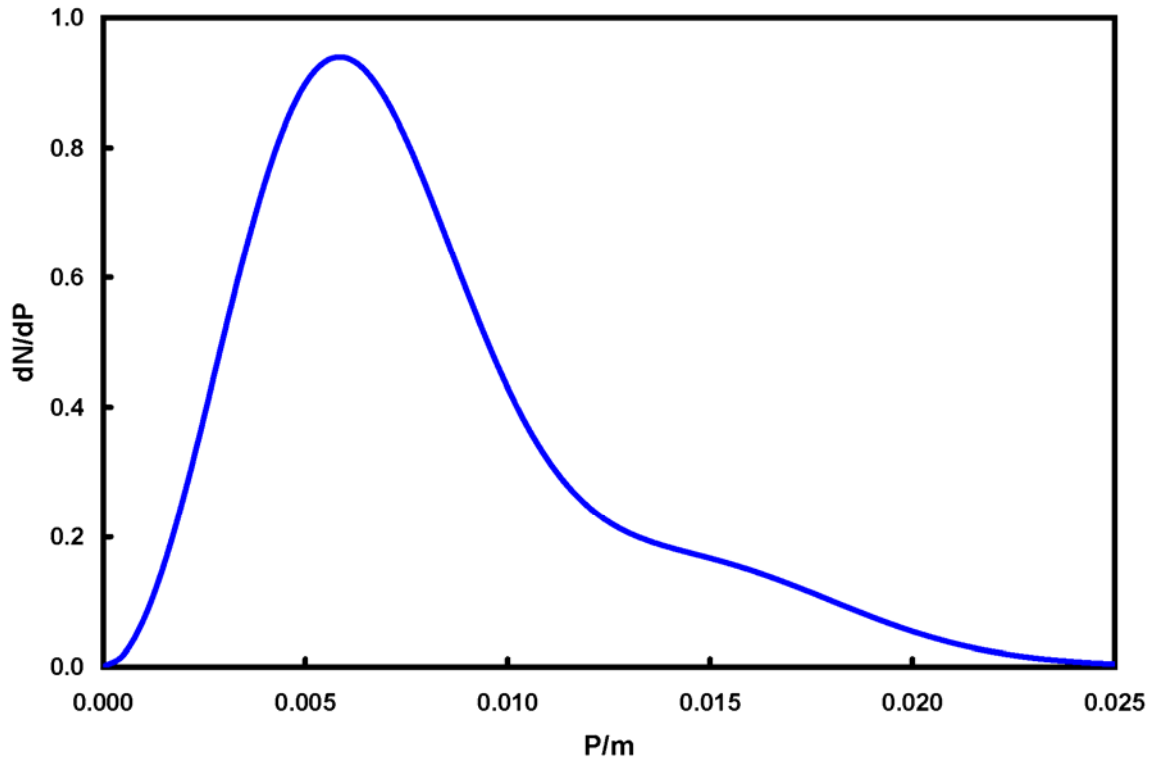


Figure 16. The momentum distribution function for positronium at annihilation as determined from the fitted curves for the 2- $\gamma$  angular correlation function.